Abdominal Radiology (2019) 44:1808–1815
https://doi.org/10.1007/s00261-019-01924-5

HEPATOBILIARY

Intra-individual comparison of conventional and simultaneous multislice-accelerated diffusion-weighted imaging in upper abdominal solid organs: value of ADC normalization using the spleen as a reference organ

Weon Jang[1] · Ji Soo Song[1,2,3] · Hyo Sung Kwak[1,2,3] · Seung Bae Hwang[1,2,3] · Mun Young Paek[4]

Published online: 8 February 2019

Abstract

Purpose To compare the apparent diffusion coefficient (ADC) value of conventional diffusion-weighted imaging (cDWI) to simultaneous multislice-accelerated DWI (sDWI) and to evaluate the possibility of ADC normalization using the spleen as a reference organ.

Methods We retrospectively evaluated 92 patients (68 men, 24 women; mean age 60.0 years) who underwent liver magnetic resonance imaging (MRI) including both cDWI and sDWI. sDWI was obtained with an acceleration factor of 2. ADC values were measured from the right liver lobe, left liver lobe, spleen, pancreas, right kidney, and left kidney. ADC values of the spleen were used for normalization. Paired sample *t* test, Pearson's correlation coefficient, and Bland–Altman method were used for statistical analysis.

Results ADC values of cDWI were significantly lower than sDWI in all six anatomic regions ($p < 0.001$). The mean difference in ADC value between cDWI and sDWI ranged from 0.048 to 0.125×10^{-3} mm^2/s. ADC values from cDWI and sDWI showed a moderate to very high positive correlation ($p < 0.001$). After ADC normalization using the spleen as a reference organ, there was no significant difference between normalized ADC of cDWI and sDWI in all 5 anatomic regions ($p = 0.11 - 0.74$).

Conclusions Normalization of ADC using the spleen could be useful for comparing upper abdominal organs acquired with either cDWI or sDWI in longitudinal and follow-up studies.

Keywords Diffusion magnetic resonance imaging · Magnetic resonance imaging · Spleen · Abdomen

Introduction

Diffusion-weighted imaging (DWI) is a functional magnetic resonance (MR) imaging technique that provides not only anatomic and structural information, but also information about the functional properties and quantitative metrics using the apparent diffusion coefficient (ADC) of the assessed tissue [1]. DWI has been proven to be a useful technique for lesion detection and characterization, for the evaluation of diffuse liver disease, and for monitoring and predicting treatment response in oncology [2–4]. Since DWI is based on the Brownian motion of water in biological tissues, it can show early functional or microstructural changes in tissue without intravenous contrast media [5–8]. In spite of its considerable diagnostic value, the relatively long scan time is a major concern that needs to be resolved if DWI is to be used more widely in daily clinical practice, especially as demand for MR imaging increases. This holds especially true for abdominal DWI, which frequently uses a respiratory-triggering technique, which often leads to long and sometimes even unpredictable scan times [9].

To reduce scan time, the simultaneous multislice (SMS) technique has been developed recently and has been reported

✉ Ji Soo Song
pichgo@gmail.com

1 Department of Radiology, Chonbuk National University Medical School and Hospital, 20 Geonji-ro, Deokjin-gu, Jeonju, Chonbuk 54907, Korea

2 Research Institute of Clinical Medicine of Chonbuk National University, Jeonju, Korea

3 Biomedical Research Institute of Chonbuk National University Hospital, Jeonju, Korea

4 Siemens Healthineers Ltd, Seoul, Korea

to provide accelerated data acquisition and reduced radiofrequency-power deposition for a broad range of MR applications [10]. It was initially introduced in brain imaging for diffusion-tensor imaging and has been successfully transferred to extracranial applications including abdominal DWI [11–13]. The SMS technique allows for reducing the scan time by the number of simultaneously excited slices, which can be determined by a SMS acceleration factor (AF) [14–18]. In addition, SMS-accelerated DWI (sDWI) of abdominal organs has presented without negative effects on signal-to-noise ratio (SNR) and with similar to or even better overall image quality [19, 20]. However, the ADC values acquired with sDWI were significantly lower than that of conventional DWI (cDWI), which is a major limitation for sDWI if it is to replace cDWI for patients, especially with follow-up studies [19, 21].

DWI with ADC measurements has been used as a quantitative biomarker for the assessment of liver fibrosis and predicting and monitoring of tumor response [8, 22–24]. Since patients eligible for the evaluation of treatment response or liver fibrosis usually undergo many follow-up studies, MR systems and sequence parameters applied may vary across different rounds of imaging. In order to use ADC values as a qualified biomarker and a prognostic parameter in longitudinal, multicenter studies, ADC measurements must be standardized. Several recent studies have shown the possibility of normalization of ADC values acquired with variable acquisition parameters or MR systems [25, 26]. Another study also used the spleen for normalization to compare ADC values from 2 different 3.0 T MR systems [27]. To the best of our knowledge, a direct comparison of ADC values and normalization of ADC values acquired from both cDWI and sDWI in a large patient cohort has not been performed previously.

The purpose of this study was to compare the ADC values of cDWI and sDWI and to evaluate the possibility of ADC normalization using the spleen as a reference organ.

Materials and methods

Study population

This retrospective study was approved by the institutional review board of our hospital, and the requirement for patient informed consent was waived for review of patient records and images. Between January 2017 and March 2017, 98 patients who underwent liver MR imaging, including both cDWI and sDWI, were retrospectively reviewed. Six patients were excluded for the following reasons: (1) severe artifacts hindering image analysis ($n=4$), (2) low SNR because of Gamna–Gandy nodules in the spleen ($n=1$), and (3) innumerable intrahepatic metastasis ($n=1$). After exclusion, liver MR imaging of 92 patients (68 men, 24 women; mean age, 60.0 years) was analyzed. Of the total patients, 39 (42.4%) had chronic hepatitis and 17 (18.5%) had liver cirrhosis.

MR imaging techniques

Liver MR imaging was performed on a 3.0 T MR system (Skyra, Siemens Healthineers) using an 18-element body matrix and 4–12 elements of integrated spine matrix coils. Both cDWI and sDWI were acquired using the free-breathing technique, and it was obtained between the 10- and 20-min hepatobiliary phase, which is acquired after dynamic bolus injection of gadoxetic acid (Gd-EOB-DTPA; Eovist; Bayer Schering Pharma, Berlin, Germany). The order of acquisition of cDWI and sDWI was randomized. An acceleration factor of 2 was used for sDWI [20]. The acquisition time was 3 min and 50 s for cDWI and 1 min and 26 s for sDWI. Detailed sequence parameters of cDWI and sDWI are summarized in Table 1.

Quantitative image analysis

Apparent diffusion coefficient maps were automatically generated on the MR system console using monoexponential fitting of all *b* values. The anatomic regions analyzed were the right and left liver lobes, spleen, pancreas, and right and left kidneys. A research personnel with 1 year of experience in quantitative image analysis drew regions of interest (ROIs) for each DWI set and each anatomic region on the $b=0$ s/mm^2 images using the picture archiving and communication system (PACS) (Maroview 5.4; Marotech). In order to place ROIs in locations

Table 1 DWI acquisition parameters

	cDWI	sDWI
Respiration control	Free breathing	Free breathing
TR/TE (ms)	6400/58	2900/61
Field of view (mm)	400 × 400	400 × 400
Matrix	128 × 128	128 × 128
Section thickness (mm)	5	5
Intersection gap (mm)	1	1
No. of sections	34	34
No. of signals acquired	4	4
b values (s/mm^2)	0, 50, 400, 800	0, 50, 400, 800
Bandwidth (Hz per pixel)	2442	2442
Parallel acceleration factor	GRAPPA = 2	GRAPPA = 2
SMS AF	N/A	2
Fat saturation	SPAIR	SPAIR
Acquisition time	3:50	1:26

cDWI conventional DWI, *sDWI* simultaneous multislice DWI, *TR/TE* repetition time/echo time, *GRAPPA* generalized auto-calibrating partially parallel acquisition, *SMS* AF simultaneous multislice acceleration factor, *N/A* not available, *SPAIR* spectral selection attenuated inversion recovery

as similar as possible between the images, 2 image sets for each subject were viewed side-by-side with a dual-monitor display. According to anatomic region and patient, the sizes of the ROIs were variable while excluding vessels and artifacts, but were as constant as possible between 2 image sets for each patient (range 2–4 cm^2 for the pancreas and kidney, and 4–8 cm^2 for the liver and spleen). ROIs were identically positioned on corresponding ADC maps by applying the copy and paste functions of the PACS system. For the right and left liver lobes, 2 ROIs from 3 contiguous slices were measured with a central section obtained through the level of the right portal vein for the right lobe and umbilical portion of the left portal vein for the left lobe. For the spleen, 2 ROIs from 3 contiguous slices were measured with a central section obtained through the level of the splenic hilum. For the pancreas, 2 ROIs including the head, body, and tail of the pancreas were obtained. For better accuracy, magnification of DWI was used, since the pancreas is a particularly difficult organ to measure. The ROIs of both kidneys were measured on 3 contiguous slices with 2 ROIs, with a central section obtained through the level of the mid-pole. A total of 72 ROIs were drawn per patient (each 6 ROIs from the 6 anatomic regions, measured in both cDWI and sDWI). All the ROIs were copied to the corresponding ADC maps. However, 12 ROIs were not obtained due to an atrophic change of the left kidney (6 ROIs in 1 patient) or an atrophic change of the pancreas (6 ROIs in 1 patient).

For non-normalized ADC, the values are absolute; however, with normalized ADC, the values are relative and are represented by a ratio. Normalized ADC has the potential to deliver a higher degree of standardization across different devices or with different parameters as normalization may minimize these differences. For normalization in this study, ADC values of 5 anatomic regions were divided by the ADC values of the spleen (ADC_{spleen}) (Fig. 1).

$$\text{Normalized ADC} = \text{ADC value of anatomic region}/ADC_{spleen}.$$

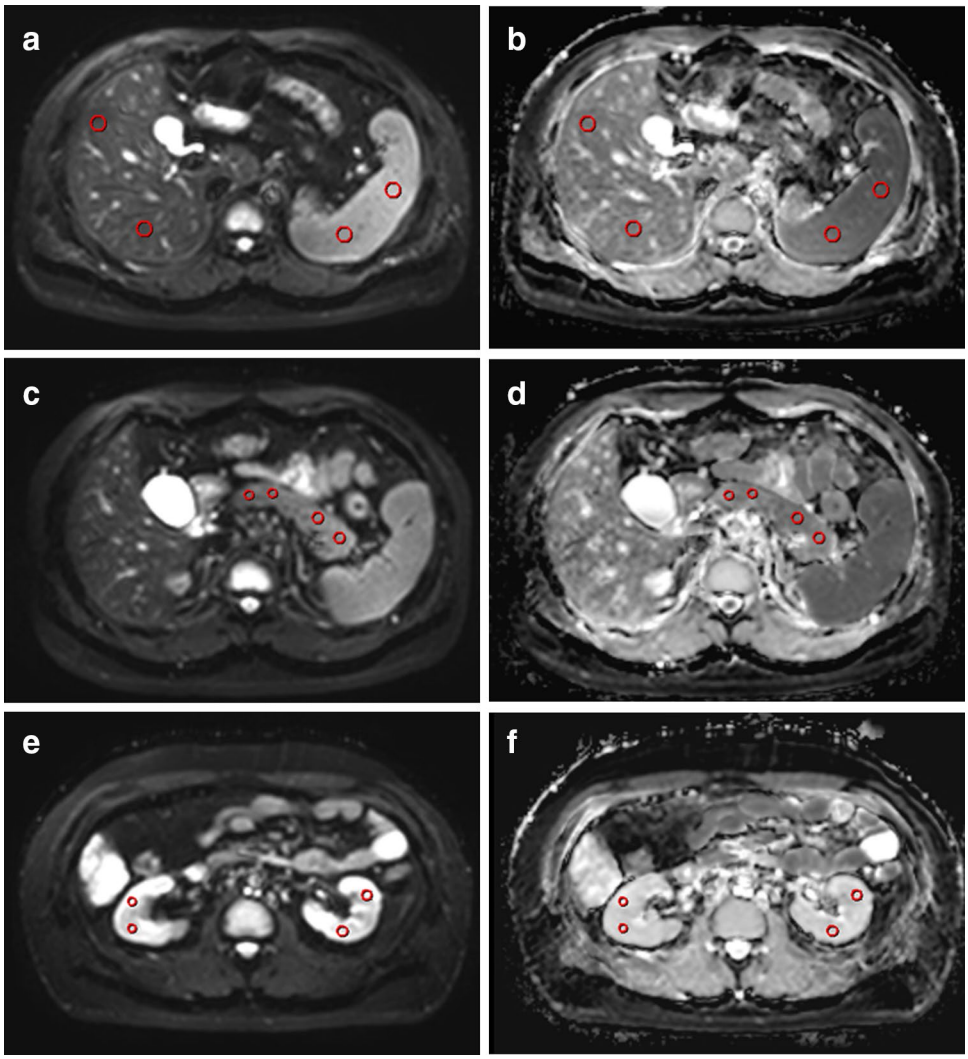

Fig. 1 Axial single-shot echo-planar simultaneous multislice-accelerated diffusion-weighted images for *b* values of 0 s/mm^2 (**a**, **c**, **e**) and apparent diffusion coefficient (ADC) maps (**b**, **d**, **f**) in a 40-year-old man with hepatic hemangioma (not shown). The region of interests for ADC measurements of 6 anatomical regions are shown as red circles

Statistical analysis

Comparison of ADC values of cDWI and sDWI of 6 anatomic regions, before and after normalization, were analyzed using the paired sample *t* test. The Pearson's correlation coefficient was used for analyzing associations for different imaging acquisition techniques, and the correlation coefficient *r* was interpreted as follows: 0.00 to 0.30, negligible correlation; 0.30 to 0.50, low positive correlation; 0.50 to 0.70, moderate positive correlation; 0.70 to 0.90, high positive correlation; 0.90 to 1.00, very high positive correlation [28]. The Bland–Altman method was used to evaluate the agreement and systematic bias of ADC values acquired with cDWI and sDWI. Statistical analysis was performed using R statistical and computing software (Version 3.4.3; http://www.r-project.org/). Results with *p* values less than 0.05 were considered to indicate a significant difference.

Results

Comparison of ADC values

Apparent diffusion coefficient values of the sDWI were significantly lower than cDWI for all 6 anatomic regions ($p < 0.001$). The right kidney showed the highest ADC value [$(2.029 \pm 0.127) \times 10^{-3}$ mm^2/s] and the spleen showed the lowest ADC value [$(0.917 \pm 0.094) \times 10^{-3}$ mm^2/s] on cDWI. On sDWI, the left kidney revealed the highest ADC value [$(1.948 \pm 0.126) \times 10^{-3}$ mm^2/s] and the spleen showed the lowest ADC value [$(0.870 \pm 0.088) \times 10^{-3}$ mm^2/s]. Apparent diffusion coefficient values from cDWI and sDWI showed a moderate to very high positive correlation with *r* ranging from 0.6997 to 0.9096 ($p < 0.001$, Table 2).

The mean difference of ADC value from Bland–Altman analysis demonstrated lower ADC values with sDWI compared to cDWI (ranging from −3.7 to −9.6%). The mean bias in ADC between the 2 sequences varied between 0.048 and 0.125×10^{-3} mm^2/s. The limits of agreement (LOA) in percentage from the Bland–Altman method was in the range of −9.3 to 23.7% for 6 anatomical regions (Fig. 2).

Comparison of ADC values after normalization

After normalization, there were no significant differences between cDWI and sDWI for all 5 anatomic regions ($p = 0.11$ − 0.74). Normalized ADC of cDWI and sDWI showed a moderate to high positive correlation, ranging from 0.7628 to 0.8772 ($p < 0.001$, Table 3).

Table 2 Comparison of ADC values between cDWI and sDWI

	cDWI	sDWI	*r**	*p*†
Right liver lobe ($n = 92$)	1.203 ± 0.090	1.147 ± 0.099	0.7019	< 0.001
Left liver lobe ($n = 92$)	1.285 ± 0.129	1.203 ± 0.127	0.7205	< 0.001
Spleen ($n = 92$)	0.917 ± 0.094	0.870 ± 0.088	0.7342	< 0.001
Pancreas ($n = 91$)	1.372 ± 0.218	1.248 ± 0.213	0.9096	< 0.001
Right kidney ($n = 92$)	2.029 ± 0.127	1.932 ± 0.119	0.7056	< 0.001
Left kidney ($n = 91$)	2.022 ± 0.133	1.948 ± 0.126	0.6997	< 0.001

Data are mean ADC value (in $\times 10^{-3}$ mm^2/s) ± standard deviation

*Pearson's correlation coefficient *r*. *p* value of all seven anatomic regions was < 0.005

†Paired samples *t* test

Discussion

Previous studies regarding SMS technique have proven that dramatic scan time reduction of up to 62% could be achieved without degradation in image quality. We used an AF of 2 because a previous study compared an AF of 2 with an AF 3, and when increasing AF to 3, it resulted in a significant deterioration in image quality. Even though another study showed that SNR remained in an acceptable range at an AF of 3, that result was only confined to skeletal muscle [29]. At the moment, most studies on the abdomen considered an AF of 2 to be the best compromise between ADC quantification accuracy, scan time, and image quality [19, 20, 30]. Despite favorable results, these studies were based on rather small cohorts of volunteers or a limited number of patients focusing on only 1 or 2 organs in particular. Our study included 92 consecutive patients with clinical liver MR imaging and analyzed 6 anatomic regions in order to compare the ADC of cDWI and sDWI. In addition, since the ADC values acquired with sDWI were significantly lower than that of cDWI, we used the spleen as a reference organ for normalization. As a result, the normalized ADCs of cDWI and sDWI did not differ significantly.

Since many recent studies have proven acceptable image quality with significant scan time reduction using sDWI, we only focused on quantitative evaluation of ADC values and its normalization, rather than analyzing image quality differences. In order to use ADC as a quantitative imaging biomarker in both research and clinical practice, standardization and optimization of DWI acquisition techniques are required. Since the reproducibility of ADC has been shown with phantoms and in the upper abdomen of both volunteers and patients, reliability in the interpretation of ADC values

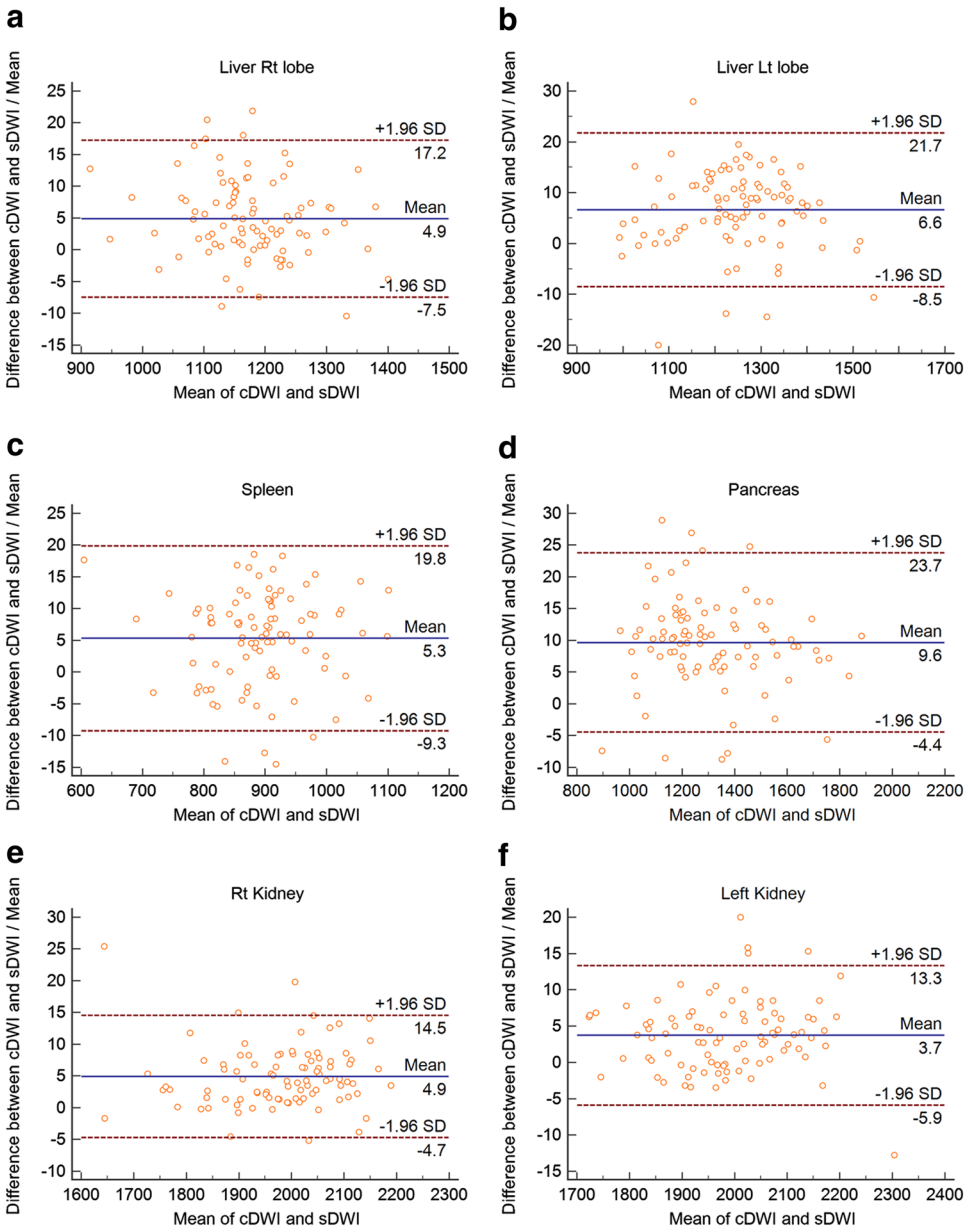

Fig. 2 Bland–Altman plots of differences as percentage of the ADC values of cDWI and sDWI (*y*-axis) in 6 anatomic regions against the mean ADC value of cDWI and sDWI (*x*-axis) with the mean absolute difference (solid line) and 95% confidence interval of the mean difference (limits of agreement) as dashed lines. Right liver lobe (**a**), left liver lobe (**b**), spleen (**c**), pancreas (**d**), right kidney (**e**), and left kidney (**f**)

from variable acquisition techniques is now required for longitudinal, multicenter studies [31–34].

A recent study presented a possibility for normalizing ADC values at 3.0 T for upper abdominal organs [27]. The spleen was used as a reference organ in the comparison of 2 different 3.0 T MR systems using a single patient cohort. DWI acquisition parameters were matched to be as identical as possible. The result was that, despite a moderate positive correlation, the ADC values between the 2 MR systems were significantly different. However, after normalization, the normalized ADC values were not significantly different, with a moderate to high positive correlation. The study suggested that normalizing ADC values of upper abdominal organs using the spleen could minimize variability between different MR systems. Since sDWI has been proven to be a useful technique to replace cDWI with a much shorter scan time, even though the ADC values differed significantly, we hypothesized that it may be possible and useful to normalize ADC values acquired with cDWI and sDWI.

Although direct comparison of the mean ADC of the current study with that of other studies might be inappropriate, it is noteworthy that the mean ADC of the spleen was in the range of previous studies [$0.762 - 0.916 \times 10^{-3}$ mm^2/s vs. $(0.806 \pm 0.124) \times 10^{-3}$ mm^2/s, respectively] [27, 35]. The highest normalized ADC was obtained for the kidneys (2.22–2.26 vs. 2.214–2.251, mean of the current study versus mean of previous study, respectively), and the right liver lobe showed the lowest normalized ADC (1.32–1.33

Table 3 Comparison of Normalized ADC Values Between cDWI and sDWI

	cDWI	sDWI	r*	$p^{\dagger}$
Right liver lobe ($n=92$)	1.32 ± 0.133	1.33 ± 0.153	0.7628	0.73
Left liver lobe ($n=92$)	1.41 ± 0.182	1.39 ± 0.183	0.8248	0.50
Pancreas ($n=91$)	1.50 ± 0.257	1.44 ± 0.262	0.8772	0.11
Right kidney ($n=92$)	2.23 ± 0.223	2.24 ± 0.249	0.7980	0.74
Left kidney ($n=91$)	2.22 ± 0.229	2.26 ± 0.240	0.7649	0.31

Data are mean ± standard deviation

*Pearson's correlation coefficient r. p value of all 5 anatomic regions was < 0.005

†Paired samples t test

vs. 1.303–1.348). Since most patients in both studies had chronic liver disease, the normalization of ADC values using the spleen in chronic liver disease patients could serve as an imaging biomarker for longitudinal and follow-up studies.

The paraspinal muscle was excluded as a reference organ, as its lower variability in ADC can be a function of it being less affected by diffusion-related parameters and its relative stability across various DWI acquisition methods. To be appropriate as a reference, the comparison organ must be affected by diffusion-related parameters in similar ways as the target organ and/or lesion. Most abdominal organs are highly perfused, having a rich vascular supply; thus, they are significantly affected by diffusion-related parameters, such as vendor-specific MR platforms, diffusion gradients, acquisition methods, such as respiratory motion-compensation techniques, and most importantly, the choice of b values. Additionally, a recent study on this issue showed that the paraspinal muscle was not appropriate as a reference organ [35]. Furthermore, the spleen is often included in liver and abdominal MR imaging, is less susceptible to systemic disease, and is highly perfused [26, 36, 37].

There are some conflicting results regarding the ADC values obtained with sDWI being lower than cDWI. Obele et al. demonstrated that there was no significant difference in liver ADCs, but the ADC obtained with sDWI was lower than cDWI on 3 T [13]. Another study also showed that there was no significant difference in ADC of the right liver and kidney obtained with cDWI and sDWI on 1.5 T [38]. Two other studies revealed that liver ADC values were significantly lower in sDWI compared to cDWI [19, 30]. Most previous studies involved a 1.5 T MR system and consisted of a small number of volunteers or less than 50 patients. In contrast, the current study was based on a 3.0 T MR system with a large number of consecutive patients in a routine clinical practice. Although not clearly proven yet, we carefully assume that the shorter TR (2900 ms) used in sDWI compared to cDWI (6400 ms) might be a factor in decreasing ADC values [13, 19]. The lower TR may lead to a reduced signal due to T1 saturation effects, especially when applying higher b values. In addition, the effect of a low TR is expected to be more distinct in free-breathing acquisitions, which may add to the tendency of lower ADC values observed in free breathing [19]. In addition, we acquired both cDWI and sDWI after the injection of gadoxetic acid, which might have an effect on ADC values, while previous studies did not. Acquiring DWI after contrast injection is more practical and increases clinical robustness. It has been proven that cDWI can be acquired after gadoxetic acid injection for up to 20 min [39, 40]. However, the effect of gadoxetic acid on sDWI has not been proven, so further study is required for verification.

Our study had several limitations. First, the retrospective nature of this current study may have biased our result. Second, we did not evaluate the image quality because several recent studies have revealed that the image quality of sDWI was similar to or even better than cDWI [20, 30]. Third, there was a lack of lesion analysis due to the small number of patients with adequate lesions. Fourth, we did not use the paraspinal muscle as a reference organ. Although a recent study with cDWI showed that the paraspinal muscle may be inappropriate as a reference organ, further study with sDWI is warranted. Fifth, we acquired both cDWI and sDWI after the administration of gadoxetic acid, although the effect of gadoxetic acid in DWI can be ignored for up to 20 min post-injection [39, 40].

In conclusion, the SMS technique is a promising approach for scan time reduction in DWI of the upper abdomen. The lower ADC in sDWI compared to cDWI could be resolved by ADC normalization using the spleen as a reference organ. This could motivate adoption of sDWI as a replacement for cDWI in abdominal imaging and provide a useful quantitative biomarker that both save time and maintain reliability.

Acknowledgements The authors thank Wade Martin of Emareye Medical Editing Service for his assistance in editing the article.

Funding None to be declared by any of the authors.

References

1. Patterson DM, Padhani AR, Collins DJ. Technology insight: water diffusion MRI--a potential new biomarker of response to cancer therapy. Nat Clin Pract Oncol. 2008;5(4):220-33.
2. Bharwani N, Koh DM. Diffusion-weighted imaging of the liver: an update. Cancer imaging : the official publication of the International Cancer Imaging Society. 2013;13:171-85.
3. Wagner M, Doblas S, Daire JL, Paradis V, Haddad N, Leitao H, et al. Diffusion-weighted MR imaging for the regional characterization of liver tumors. Radiology. 2012;264(2):464-72.

4. Bains LJ, Zweifel M, Thoeny HC. Therapy response with diffusion MRI: an update. Cancer Imaging. 2012;12:395-402.
5. Taouli B, Koh DM. Diffusion-weighted MR imaging of the liver. Radiology. 2010;254(1):47-66.
6. Koh DM, Collins DJ. Diffusion-weighted MRI in the body: applications and challenges in oncology. AJR Am J Roentgenol. 2007;188(6):1622-35.
7. Thoeny HC, De Keyzer F. Extracranial applications of diffusion-weighted magnetic resonance imaging. Eur Radiol. 2007;17(6):1385-93.
8. Parikh T, Drew SJ, Lee VS, Wong S, Hecht EM, Babb JS, et al. Focal liver lesion detection and characterization with diffusion-weighted MR imaging: comparison with standard breath-hold T2-weighted imaging. Radiology. 2008;246(3):812-22.
9. Jerome NP, Orton MR, d'Arcy JA, Collins DJ, Koh DM, Leach MO. Comparison of free-breathing with navigator-controlled acquisition regimes in abdominal diffusion-weighted magnetic resonance images: Effect on ADC and IVIM statistics. J Magn Reson Imaging. 2014;39(1):235-40.
10. Barth M, Breuer F, Koopmans PJ, Norris DG, Poser BA. Simultaneous multislice (SMS) imaging techniques. Magn Reson Med. 2016;75(1):63-81.
11. Filli L, Ghafoor S, Kenkel D, Liu W, Weiland E, Andreisek G, et al. Simultaneous multi-slice readout-segmented echo planar imaging for accelerated diffusion-weighted imaging of the breast. Eur J Radiol. 2016;85(1):274-78.
12. Lau AZ, Tunnicliffe EM, Frost R, Koopmans PJ, Tyler DJ, Robson MD. Accelerated human cardiac diffusion tensor imaging using simultaneous multislice imaging. Magn Reson Med. 2015;73(3):995-1004.
13. Obele CC, Glielmi C, Ream J, Doshi A, Campbell N, Zhang HC, et al. Simultaneous Multislice Accelerated Free-Breathing Diffusion-Weighted Imaging of the Liver at 3T. Abdom Imaging. 2015;40(7):2323-30.
14. Xu J, Moeller S, Auerbach EJ, Strupp J, Smith SM, Feinberg DA, et al. Evaluation of slice accelerations using multiband echo planar imaging at 3 T. Neuroimage. 2013;83:991-1001.
15. Moeller S, Yacoub E, Olman CA, Auerbach E, Strupp J, Harel N, et al. Multiband multislice GE-EPI at 7 tesla, with 16-fold acceleration using partial parallel imaging with application to high spatial and temporal whole-brain fMRI. Magn Reson Med. 2010;63(5):1144-53.
16. Feinberg DA, Moeller S, Smith SM, Auerbach E, Ramanna S, Gunther M, et al. Multiplexed echo planar imaging for sub-second whole brain FMRI and fast diffusion imaging. PLoS One. 2010;5(12):e15710.
17. Van Essen DC, Ugurbil K, Auerbach E, Barch D, Behrens TE, Bucholz R, et al. The Human Connectome Project: a data acquisition perspective. Neuroimage. 2012;62(4):2222-31.
18. Auerbach EJ, Xu J, Yacoub E, Moeller S, Ugurbil K. Multiband accelerated spin-echo echo planar imaging with reduced peak RF power using time-shifted RF pulses. Magn Reson Med. 2013;69(5):1261-7.
19. Taron J, Martirosian P, Erb M, Kuestner T, Schwenzer NF, Schmidt H, et al. Simultaneous multislice diffusion-weighted MRI of the liver: Analysis of different breathing schemes in comparison to standard sequences. J Magn Reson Imaging. 2016;44(4):865-79.
20. Taron J, Martirosian P, Kuestner T, Schwenzer NF, Othman A, Weiss J, et al. Scan time reduction in diffusion-weighted imaging of the pancreas using a simultaneous multislice technique with different acceleration factors: How fast can we go? Eur Radiol. 2018;28(4):1504-11.
21. Kenkel D, Barth BK, Piccirelli M, Filli L, Finkenstadt T, Reiner CS, et al. Simultaneous Multislice Diffusion-Weighted Imaging of the Kidney: A Systematic Analysis of Image Quality. Invest Radiol. 2017;52(3):163-69.
22. Koh DM, Scurr E, Collins D, Kanber B, Norman A, Leach MO, et al. Predicting response of colorectal hepatic metastasis: value of pretreatment apparent diffusion coefficients. AJR American journal of roentgenology. 2007;188(4):1001-8.
23. Low RN, Gurney J. Diffusion-weighted MRI (DWI) in the oncology patient: value of breathhold DWI compared to unenhanced and gadolinium-enhanced MRI. Journal of magnetic resonance imaging : JMRI. 2007;25(4):848-58.
24. Bruegel M, Holzapfel K, Gaa J, Woertler K, Waldt S, Kiefer B, et al. Characterization of focal liver lesions by ADC measurements using a respiratory triggered diffusion-weighted single-shot echo-planar MR imaging technique. European radiology. 2008;18(3):477-85.
25. Padhani AR, Liu G, Koh DM, Chenevert TL, Thoeny HC, Takahara T, et al. Diffusion-weighted magnetic resonance imaging as a cancer biomarker: consensus and recommendations. Neoplasia. 2009;11(2):102-25.
26. Papanikolaou N, Gourtsoyianni S, Yarmenitis S, Maris T, Gourtsoyiannis N. Comparison between two-point and four-point methods for quantification of apparent diffusion coefficient of normal liver parenchyma and focal lesions. Value of normalization with spleen. Eur J Radiol. 2010;73(2):305-9.
27. Song JS, Hwang SB, Chung GH, Jin GY. Intra-Individual, Inter-Vendor Comparison of Diffusion-Weighted MR Imaging of Upper Abdominal Organs at 3.0 Tesla with an Emphasis on the Value of Normalization with the Spleen. Korean J Radiol. 2016;17(2):209-17.
28. Hinkle De WWJSG. Applied statistics for the behavioral sciences, 5th ed 2003.
29. Filli L, Piccirelli M, Kenkel D, Guggenberger R, Andreisek G, Beck T, et al. Simultaneous Multislice Echo Planar Imaging With Blipped Controlled Aliasing in Parallel Imaging Results in Higher Acceleration: A Promising Technique for Accelerated Diffusion Tensor Imaging of Skeletal Muscle. Invest Radiol. 2015;50(7):456-63.
30. Taron J, Martirosian P, Schwenzer NF, Erb M, Kuestner T, Weiss J, et al. Scan time minimization in hepatic diffusion-weighted imaging: evaluation of the simultaneous multislice acceleration technique with different acceleration factors and gradient preparation schemes. MAGMA. 2016;29(5):739-49.
31. Braithwaite AC, Dale BM, Boll DT, Merkle EM. Short- and midterm reproducibility of apparent diffusion coefficient measurements at 3.0-T diffusion-weighted imaging of the abdomen. Radiology. 2009;250(2):459-65.
32. Koh DM, Blackledge M, Collins DJ, Padhani AR, Wallace T, Wilton B, et al. Reproducibility and changes in the apparent diffusion coefficients of solid tumours treated with combretastatin A4 phosphate and bevacizumab in a two-centre phase I clinical trial. Eur Radiol. 2009;19(11):2728-38.
33. Corona-Villalobos CP, Pan L, Halappa VG, Bonekamp S, Lorenz CH, Eng J, et al. Agreement and reproducibility of apparent diffusion coefficient measurements of dual-b-value and multi-b-value diffusion-weighted magnetic resonance imaging at 1.5 Tesla in phantom and in soft tissues of the abdomen. J Comput Assist Tomogr. 2013;37(1):46-51.
34. Miquel ME, Scott AD, Macdougall ND, Boubertakh R, Bharwani N, Rockall AG. In vitro and in vivo repeatability of abdominal diffusion-weighted MRI. Br J Radiol. 2012;85(1019):1507-12.
35. Song JS, Kwak HS, Byon JH, Jin GY. Diffusion-weighted MR imaging of upper abdominal organs at different time points: Apparent diffusion coefficient normalization using a reference organ. Journal of magnetic resonance imaging : JMRI. 2017;45(5):1494-501.

36. Do RK, Chandarana H, Felker E, Hajdu CH, Babb JS, Kim D, et al. Diagnosis of liver fibrosis and cirrhosis with diffusion-weighted imaging: value of normalized apparent diffusion coefficient using the spleen as reference organ. AJR Am J Roentgenol. 2010;195(3):671-6.
37. Kim T, Murakami T, Takahashi S, Hori M, Tsuda K, Nakamura H. Diffusion-weighted single-shot echoplanar MR imaging for liver disease. AJR Am J Roentgenol. 1999;173(2):393-8.
38. Taron J, Weiß J, Martirosian P, Seith F, Stemmer A, Bamberg F, et al. Clinical Robustness of Accelerated and Optimized Abdominal Diffusion-Weighted Imaging. Investigative Radiology. 2017;52(10):590-95.
39. Kinner S, Umutlu L, Blex S, Maderwald S, Antoch G, Ertle J, et al. Diffusion weighted MR imaging in patients with HCC and liver cirrhosis after administration of different gadolinium contrast agents: is it still reliable? Eur J Radiol. 2012;81(4):e625-8.
40. Colagrande S, Mazzoni LN, Mazzoni E, Pradella S. Effects of gadoxetic acid on quantitative diffusion-weighted imaging of the liver. J Magn Reson Imaging. 2013;38(2):365-70.